Climate as a complex, self-regulating system

Supplementary Information

Roger N Jones and James H Ricketts

S1. Methods

The analyses presented in this SI were carried out with those in a companion paper (Jones and Ricketts, 2021) and some of the supporting information is contained in the SI for that paper. Cross-references will be made when appropriate.

S1.1. Climate model analyses

S1.1.1. Shift detection

Shift detection was carried out using the multistep bivariate test (Ricketts, 2015;Jones and Ricketts, 2017;Ricketts and Jones, 2018;Ricketts, 2019) and an extensive assessment of its performance is provided in the accompanying SI, largely drawn from Ricketts (2019).

SST for the TEP and TWP regions was extracted from 30 coupled atmosphere-ocean GCMs from the CMIP5 database, RCP4.5 ensemble run 1 physical representation 1. This data was matched with 29 available records of GMST from JR17 and 27 estimates of equilibrium climate sensitivity (ECS) from the literature. These were analysed using the multistep bivariate test and the results are summarised in Section S2.

S1.1.2. Probability testing

The likelihood of shifts in TWP and TEP matching shifts in GMST ±1 year for the 29 models was calculated for no area weighting, and TEP and TWP as comprising 5.7% of the global and 14.25% of the tropical region. The method draws shift years for each model for TWP and TEP, and assess likelihood of them coinciding with the available shifts in GMST, initially over the entire 240-year period 1861–2100. There is no probability attached to the appearance of a shift or allowance for variations in forcing over time; instead, likelihoods are calculated after the fact. The procedure is: given *i* shifts in TWP and TEP and *j* shifts in GMST, calculate the probability of shifts 1 to *i* coinciding with shifts 1 to *j* ±1 year. Given that weighting over time would result in some clustering, this procedure assumes that given shifts occur the process generating their frequency and timing is random. We also overlap TWP and TEP, treating them as one area adjusting the 3-year window if that is the case. For example, if there are 11 shifts with one overlapping by a year, the total window is 31 years. Each match retires 7 years from the total timeseries of 240 years. This procedure was carried out for the 29 models with available data. The outcome for observations is p=0.049, because some of the contributing shifts in TEP and TWP precede GMST by more than a year. The test for observations covers 1880–2018, whereas the model analyses proceed through a period of increasing forcing to around 2060. Because the causal assumption is that TWP and TEP influence GMST, the ±1 year window represents sampling uncertainty and the causal response is expected lie within that. However, as seen from observations the initial shift may precede that in GMST by more than a year. These probabilities are therefore calculated using simplified assumptions that are stricter than those that would be encountered if observations are held to be the rule.

S1.1.3. Tracking model

The tracking model used on observations is described in the SI of the accompanying paper (Section S2.1). The same exercise has been carried out for three models: CESM1-CAM5, NorESM1-M and MIROC-ESM. The tracking model follows the cumulative running mean for TWP to assess whether a regime shift has occurred and whether it coincides with a running six-month average above a threshold set by trial and error. Similar tracking is carried out for TEP but without the exceedance test because of the volatile nature of the TEP record. TWP acts as an accumulating heat store whereas TEP acts as a heat transfer station.

Data from ten regions was analysed: TWP, TEP, GMST, global land, global ocean, tropical ocean (20 °S–20 °N, SH 30–60 °S, NH 30–60 °N, NH land and SH land. These were selected as the ten most important regions thermodynamically based in the analyses in JR21. Step changes were assessed manually on an annual and monthly basis to pinpoint shift dates. The criteria for annual changes is p<0.01, but the timing of monthly changes associated with a particular date takes precedence, sometimes leading to an adjustment in the detected year.

S1.1.4. Granger analysis

A Granger regression analysis was used to perform two-way lagged regression analysis between TWP, TEP and GMST, for the three GCMs tested for tracking. The results are compared with observations in the main paper. Testing was carried out using the Real Statistics resource pack Release 6.3 (Zaiontz, 2018). Both de-stepped (stationary) and the raw data was tested, but only the results from the raw data are shown in the main paper. Using nonstationary time series invalidates p-values, but the f-test results are of most interest. Observations are tested in both stationary and non-stationary form in JR21, so we are confident the nonstationary results presented here represent the timing, direction and strength of warming during regime shifts.

http://www.real-statistics.com/free-download/real-statistics-resource-pack/

S2. Results

S2.1. Multi-step bivariate tests

The results of the error checking accompanying the MSBV results for TWP and TEP are presented in Table S1. The interpretive information for these is in Table S2 of the SI of the companion paper. The results show that TEP is overwhelmingly *single, stationary*. TWP contains 15% *nonstationary* shifts, showing more complicated behaviour. The earliest *nonstationary* shift in TEP is 2020, and in TWP is 1997. There are no single *nonstationary* shifts in TEP but TWP registers 15 in the historical period and 21 after 2020. The ANCOVA $p<0.05$ threshold is shown in Table S1. TEP performs slightly better than TWP, with 69% $p<0.05$ and 61% $p<0.05$ respectively. For both, 3% of the balance of probabilities do not favour a breakpoint, while the rest do.

Table S1: Results of the analysis of data segments based on post-detection tests from 30 climate models and one set of observations ERSSTv5 for TEP and TWP. Note: this also contains observations, which are all single stationary.

Area	Classification of Change	ANCOVA p<0.05	Count	Totals
TEP	Single, Stationary	Yes	82	
TEP	Single, Stationary	No	37	119
TEP	Multiple, Stationary	Yes	1	
TEP	Multiple, Stationary	No	0	1
TEP	Single, N/A	Yes	0	
TEP	Single, N/A	No	0	0
TEP	Single, Nonstationary	Yes	3	
TEP	Single, Nonstationary	No	0	3
TEP	Nonstationary	Yes	1	
TEP	Nonstationary	No	0	1
Total				124
TWP	Single, Stationary	Yes	113	
TWP	Single, Stationary	No	34	145
TWP	Multiple, Stationary	Yes	25	
TWP	Multiple, Stationary	No	4	29
TWP	Single, N/A	Yes	14	
TWP	Single, N/A	No	11	25
TWP	Single, Nonstationary	Yes	25	
TWP	Single, Nonstationary	No	11	36
TWP	Nonstationary	Yes	8	
TWP	Nonstationary	No	1	6
Total				246

The gradient between TWP and TEP varies widely amongst models but remains relatively constant over time as shown in Figure S1. This is a robust aspect of the heat-pump structure as is the ratio between shift size and frequency between east and west, discussed in Section 3.3.1 of the main paper.

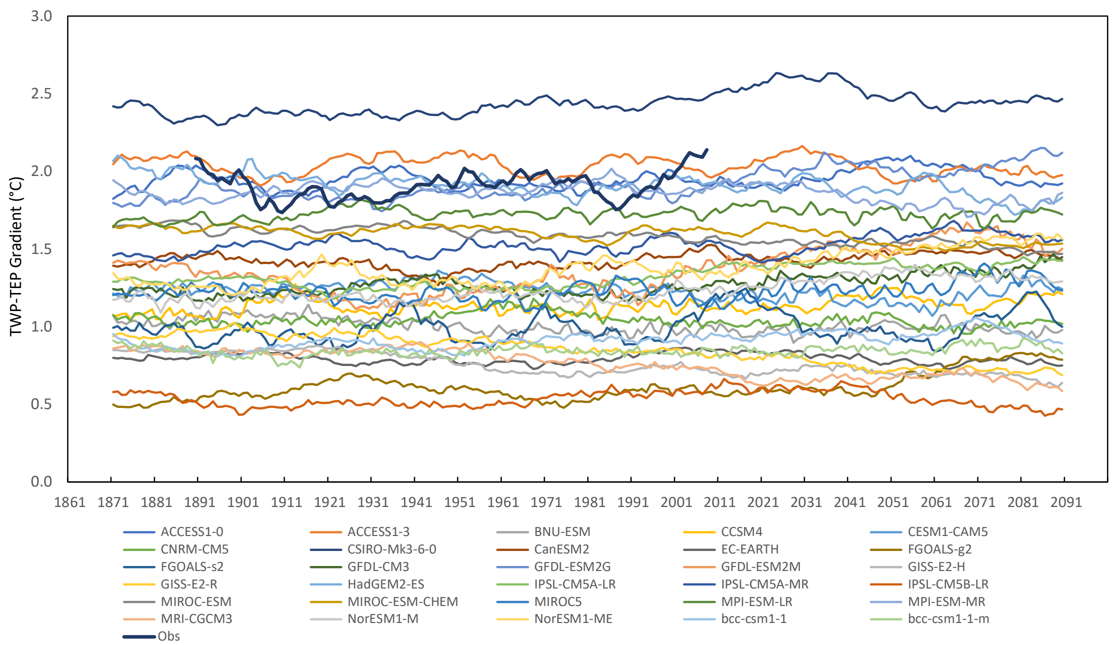

Figure S1: Gradients between TWP and TEP for 30 RCP4.5 GCMs shown with observations.

Shift-to-total-warming ratios for TEP and TWP are dominated by shifts over internal trends. Six ratios are <0.5 for TEP and three for TWP while in most, shifts dominate. TEP varies more widely, while the mode for TWP centres is 0.8 (Figure S3). Ratios above 1 indicates that sea surface temperatures (SST) are cooling between shifts in warming. The reduced variation within TWP is interpreted as a tighter geographic control of the warm pool by landmasses within models, whereas the placement of the core ENSO and cold tongue areas are likely to vary more widely.

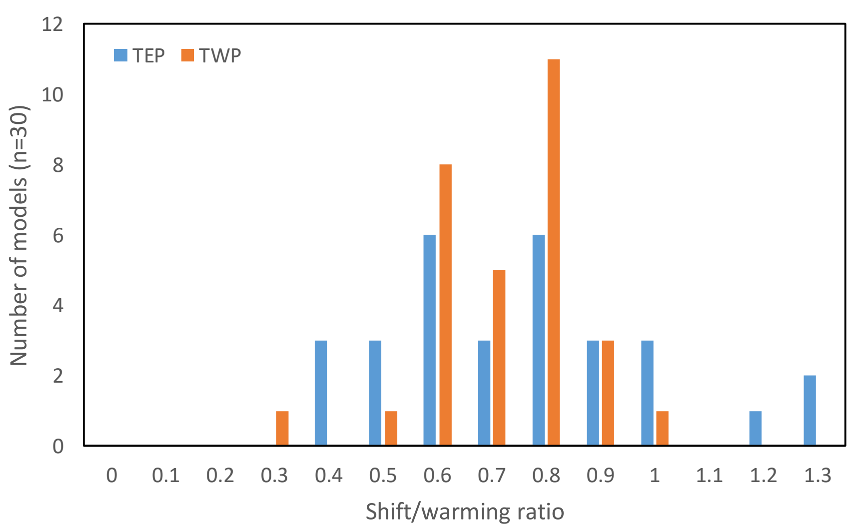

Figure S2: Distribution of shift to total warming ratios for 30 RCP4.5 GCMs for TEP and TWP.

S2.2. Relationships with GMST

In matching shifts in TWP and TEP with GMST, the unweighted case assumes that shifts from two regions of 5.7% in global area have a direct influence on global shifts. Probabilities compared to the null case range from 0.43 to 0.0005, averaging 0.15 and median 0.10, with eight models under p=0.05. When area-weighted for the proportion of TWP or TEP in total global surface area, all results are p<0.05. If we assume that changes are triggered in the tropics only, the area-adjusted probabilities result in 25 of 29 models lower than observations and the p<0.05 threshold (Table S2). The detailed results are shown in Table S9. Table S3 shows the basic results from the average values of TEP and TWP from the model ensemble regressed to estimate ECS, based on observations.

Table S2: Probabilities of matching shifts in TEP and TWP with GMST.

Model	No weighting	Area-weighted global	Area-weighted tropics	TEP average	TWP average
ACCESS1-0	0.29	0.02	0.04	0.51	0.26
ACCESS1-3	0.09	0.01	0.01	0.65	0.26
bcc-csm1-1	0.26	0.01	0.04	0.38	0.21
bcc-csm1-1-m	0.20	0.01	0.03	0.60	0.28
BNU-ESM	0.03	0.00	0.00	0.70	0.29
CanESM2	0.007	0.00	0.00	0.58	0.31
CCSM4	0.38	0.02	0.05	0.49	0.19
CESM1-CAM5	**0.12**	0.01	0.02	0.65	0.24
CNRM-CM5	0.06	0.00	0.01	0.54	0.25
CSIRO-Mk3-6-0	0.04	0.00	0.01	0.52	0.44
EC-EARTH	0.31	0.02	0.04	0.36	0.22
FGOALS-g2	0.43	0.02	0.06	0.44	0.20
GFDL-CM3	0.16	0.01	0.02	0.55	0.29
GFDL-ESM2G	0.21	0.01	0.03	0.78	0.42
GFDL-ESM2M	0.03	0.00	0.00	0.55	0.30
GISS-E2-H	0.05	0.00	0.01	0.57	0.31
GISS-E2-R	0.42	0.02	0.06	0.30	0.24
HadGEM2-ES	0.09	0.01	0.01	0.29	0.24
IPSL-CM5A-LR	0.0005	0.00	0.00	0.61	0.28
IPSL-CM5A-MR	0.16	0.01	0.02	0.57	0.39
IPSL-CM5B-LR	0.09	0.01	0.01	0.49	0.30
MIROC5	0.36	0.02	0.05	0.50	0.27
MIROC-ESM	**0.004**	0.00	0.00	0.69	0.34
MIROC-ESM-CHEM	0.02	0.00	0.00	0.36	0.33
MPI-ESM-LR	0.03	0.00	0.00	0.40	0.32
MPI-ESM-MR	0.09	0.01	0.01	0.70	0.38
MRI-CGCM3	0.28	0.02	0.04	0.54	0.32
NorESM1-M	**0.10**	0.01	0.01	0.40	0.21
NorESM1-ME	0.14	0.01	0.02	0.38	0.25
Average	0.15	0.009	0.02	0.49	0.28
Median	0.10	0.006	0.01		
Min	0.0005	0.00003	0.0001		
Max	0.43	0.025	0.06		
Higher p than observations	21	0	4		
Lower p than observations	8	29	25		
Less than p0.01	3	19	10		
Less than p0.05	5	10	15		

Table S3: Regressed ECS from average TEP, TWP and joint TEP, TWP.

	Est ECS	SE	Adj r^2	P (f-stat)
TEP	3.2	0.60	0.30	0.002
TWP	3.2	0.67	0.12	0.05
Both	3.1	0.58	0.34	0.003

At the suggestion of a reviewer, we investigated address skill scores, which have recently become available for the CMIP5 models (Fasullo, 2020;Fasullo et al., 2020). Combining available ECS and 23 skill scores provides a sample of n=21 for testing. Correlations between selected variables from the model heat engine tests with the skill scores for the CMIP5 models are shown in Table S4. Some correlations are negative, associated with lower skill scores and are influenced by ECS. We divided the set into two groups above and below an ECS of 3.5 °C, summarised in Table S5. These are very small sample sizes, so correlations can be affected by one or two outliers. Full results in Table S10.

Table S4: Correlations between model skill (n=23) and measures of TEP, TWP and GMST performance bolded where $p<0.05$. SWR – shift warming ratio. Note ECS n=21.

	overall	**energy**	**water**	**dyna-mics**	**annual**	**seas-onal**	**ENSO**	**PRW**	**SLP**	**LWNet toa**	**Z500**	**RH500**
ECS	0.40	0.37	**0.43**	0.37	**0.50**	0.23	0.29	0.40	0.22	**0.54**	0.35	0.11
TEP av	**0.56**	**0.57**	**0.50**	**0.55**	**0.58**	**0.42**	**0.45**	**0.56**	0.29	**0.61**	**0.45**	0.35
TWP av	**-0.48**	**-0.44**	**-0.51**	**-0.42**	-0.03	-0.31	**-0.53**	-0.38	-0.33	-0.20	-0.32	**-0.56**
Diff	-0.02	-0.10	0.06	-0.07	-0.19	-0.01	-0.02	-0.07	-0.05	-0.21	-0.12	0.10
TEP shifts	**-0.75**	**-0.79**	**-0.71**	**-0.69**	**-0.53**	**-0.44**	**-0.74**	**-0.77**	**-0.52**	**-0.71**	**-0.59**	**-0.48**
TWP shifts	0.21	0.17	0.15	0.25	0.11	0.24	0.15	-0.03	0.11	0.00	0.28	0.38
TEP hits	**-0.45**	**-0.50**	**-0.43**	**-0.42**	-0.29	-0.07	**-0.54**	**-0.54**	**-0.54**	**-0.53**	**-0.48**	-0.23
TWP hits	-0.37	**-0.47**	-0.36	-0.31	-0.23	-0.24	-0.39	**-0.44**	-0.23	-0.32	-0.24	-0.26
TEP SWR	**-0.63**	**-0.69**	**-0.60**	**-0.49**	-0.12	-0.32	**-0.70**	**-0.65**	-0.23	**-0.49**	-0.32	**-0.56**
TWP SWR	-0.15	-0.26	-0.13	-0.06	0.14	0.08	-0.28	-0.27	-0.14	-0.08	-0.13	-0.02
GMST hits %	**-0.45**	**-0.51**	**-0.43**	-0.41	-0.38	-0.30	**-0.43**	**-0.50**	-0.33	**-0.43**	-0.37	-0.24
TWP&TEP hits	**-0.53**	**-0.63**	**-0.52**	**-0.46**	-0.36	-0.21	**-0.59**	**-0.63**	**-0.48**	**-0.54**	**-0.46**	-0.24
TEP/TWP ratio	**-0.79**	**-0.82**	**-0.73**	**-0.75**	**-0.53**	**-0.55**	**-0.75**	**-0.71**	**-0.49**	**-0.65**	**-0.64**	**-0.64**
TEP/TWP size	**-0.82**	**-0.80**	**-0.78**	**-0.76**	**-0.52**	**-0.58**	**-0.76**	**-0.73**	**-0.47**	**-0.64**	**-0.63**	**-0.68**
	SWNet toa	**LH**	**Usfc**	**LWcf**	**Rt-Fs**	**P**	**E-P**	**SWcf**	**Fs**	**RHsfc**	**W500**	**mean**
ECS	0.14	**0.46**	**0.49**	**0.51**	0.32	0.37	**0.45**	0.21	0.26	0.00	0.35	0.34
TEP av	0.38	**0.46**	**0.48**	**0.62**	**0.56**	0.37	**0.42**	**0.48**	0.38	0.12	**0.53**	0.47
TWP av	**-0.61**	-0.40	-0.08	-0.16	-0.27	**-0.52**	**-0.50**	**-0.55**	-0.22	-0.01	-0.34	-0.35
Diff	0.01	0.07	-0.19	-0.03	-0.18	0.19	0.14	-0.03	-0.26	-0.40	-0.06	-0.06
TEP shifts	**-0.72**	**-0.61**	**-0.42**	**-0.66**	**-0.60**	**-0.58**	**-0.60**	**-0.75**	**-0.53**	-0.16	**-0.64**	-0.61
TWP shifts	0.22	0.21	0.26	0.01	0.14	0.09	0.15	0.27	0.09	0.22	0.14	0.17
TEP hits	**-0.51**	-0.33	-0.09	**-0.43**	-0.12	-0.40	-0.38	**-0.45**	-0.33	0.00	-0.37	-0.37
TWP hits	**-0.42**	-0.32	-0.19	-0.34	-0.32	-0.23	-0.24	**-0.46**	**-0.44**	-0.22	-0.25	-0.32
TEP SWR	**-0.78**	**-0.56**	-0.26	**-0.46**	**-0.59**	**-0.49**	**-0.59**	**-0.73**	**-0.54**	0.02	**-0.46**	-0.49
TWP SWR	-0.36	-0.34	-0.22	-0.11	0.12	-0.05	-0.23	-0.31	-0.34	**0.50**	0.04	-0.11
GMST hits %	-0.40	-0.39	-0.20	-0.40	-0.28	-0.33	-0.31	**-0.47**	-0.33	-0.15	-0.39	-0.37
TWP&TEP hits	**-0.57**	**-0.48**	-0.26	**-0.50**	-0.38	-0.38	-0.39	**-0.57**	**-0.52**	-0.14	-0.40	-0.44
TEP/TWP ratio	**-0.77**	**-0.67**	**-0.51**	**-0.61**	**-0.62**	**-0.59**	**-0.63**	**-0.83**	**-0.54**	-0.23	**-0.66**	-0.64
TEP/TWP size	**-0.77**	**-0.70**	**-0.52**	**-0.60**	**-0.65**	**-0.65**	**-0.70**	**-0.82**	**-0.51**	-0.18	**-0.69**	-0.65

PRW precipitable water, SLP sea level pressure, LWNet toa, top-of-atmosphere net longwave radiation, Z500 500 hPa geopotential height, 500 hPa relative humidity, LWNet toa, top-of-atmosphere net shortwave radiation, LH latent heat, Usfc surface-adjusted windspeed, LWcf cloud-forced longwave radiation, Rt-Fs total energy input toa downward minus surface upward, P precipitation, E-P evaporation-precipitation deficit, SWcf shortwave cloud forcing, Fs surface energy flux, RHsfc surface relative humidity, W500 vertical velocity at 500 hPa. SWR shift warming ratio.

The most affected variable is TWP size, where the result is highly negative for ECS >3.5 °C and weak below. For the TWP-TEP difference, it is highly positive above >3.5 °C and weakly negative below, showing no net effect for the whole sample. The TEP shift/warming ratio (SWR) is also affected by outliers. Skill has little effect on these variables, or on the TWP SWR or number of shifts. The probabilities in Table S2 do also not correlate with skills, so are not shown. The conclusion is that the performance of these measures in TWP are not linked to model skill.

Some skill is associated with TEP, where it is positive with size and negative for the number of shifts and in both cases, slightly stronger <3.5 °C. It is also negative for the number of matches, and this is because skill is associated with fewer numbers of TEP, so the chance of getting a match is reduced slightly. There is some suggestion that greater skill in the water cycle and longwave radiation leads to higher ECS, but less so above 3.5 °C.

This is described more fully in the main text, but the highest associations between skill and heat engine performance is between the relative frequency of TEP compared to TWP and the relative size of TWP compared to TEP. These show that the relationship between TWP and TEP is an essential part of the heat engine and that it is related to model skill.

Table S5: Summary of correlations between model skill (n=23) and measures of TEP, TWP and GMST performance where p<0.05. SWR – shift warming ratio.

Measure	Skills p<0.05	Av Corr	Skills <3.5 °C	Av Corr	Skills >3.5 °C	Av Corr	Result
ECS	7	0.34	3	0.45	0	0.22	Greater skill, lower ECS. Water cycle, latent heat, geopotential height
TEP av (°C)	17	0.47	2	0.45	0	0.31	Greater skill, higher av TEP. Some partitioning by ECS each way for individual skills
TWP av (°C)	10	-0.35	0	-0.20	15	-0.69	Greater skill, lower TWP. Strongly partitioned
Diff (°C)	0	-0.06	3	-0.39	14	0.70	Greater skill, higher gradient above >3.5 °C, lower gradient <3.5 °C, no overall effect
TEP shifts (n)	22	-0.61	14	-0.62	9	-0.56	Greater skill, fewer TEP shifts. Not partitioned by ECS
TWP shifts (n)	0	0.17	0	0.26	0	0.14	No effect
TEP hits (n)	12	-0.37	8	-0.54	1	-0.29	Greater skill, fewer matches, partitioned by <3.5 °C
TWP hits (n)`	5	-0.32	0	-0.15	6	-0.51	Greater skill, fewer matches, partitioned by >3.5 °C
TEP SWR	17	-0.49	7	-0.43	6	-0.46	Greater skill, lower ratio, affected by low-skill outliers
TWP SWR	1	-0.11	0	-0.11	1	-0.05	No effect
GMST hits %	7	-0.37	0	-0.27	1	-0.39	Negative for whole sample, influenced by TEP result
TWP&TEP hits %	14	-0.44	1	-0.37	6	-0.46	Negative for whole sample, partitioned by >3.5 °C, influenced by sample size
TEP/TWP frequency	22	-0.64	13	-0.67	9	-0.59	Negative for whole sample, very strong effect
TEP/TWP size	22	-0.65	5	-0.59	15	-0.69	Negative for whole sample, weakly partitioned by ECS

S2.2.1. Tracking model results

The tracking model results are shown in Plates S1–S3. They show some relationship between peaks in TWP and shifts, but not as often as for observations. The threshold value for TWP is 0.3 °C for six months above the running mean for CESM1-CAM5 and MIROC-ESM and 0.2 °C for Nor-ESM-M. The TWP-TEP relationship is maintained throughout the sequence, with TWP leading for two models and TEP for the other, this also applies for shift initiation. Most shift sequences are initiated in in the ocean, about half in the heat engine region. More work would be needed with sampling in finer detail and numerical analysis to understand how shifts are being initiated in the models. Because the models are not as tightly coupled as observations during forced mode, their behaviour is somewhere between free and forced mode.

S2.2.2. Granger analyses

Results of the Granger analyses are shown for three periods: (1) 1880 to the first large co-ordinated shift sequence after the mid-20th century, (2) from that date to 2018 to match the observed data and (3) from the same date to 2100. The first large shift is to mimic the free to forced response seen in observations even though the models do not show the clear transitions seen in observations.

The main types of result are:

- A large lag-1 declining effect means that last year's values strongly influence this year's outcomes.
- Lag-2 peaks means that the last two years affect this year's outcomes. Acute lag-3 is the last three years.
- Longer and trailing effects can denote behaviour such as abrupt reversals in lagged correlation (e.g., with ENSO) or complex two-way circulation.

The de-stepped results are shown in Fig. S3 and the raw results are shown in Fig. 3 of the main paper. The best result is for the influence of TEP on GMST where CESM1-CAM5 gets the shape right but is too weak. The models overemphasise the effect of TEP on TWP, which means that the two-way coupling between the two is weak and the flow from TEP to TWP too dominant.

Figure S3: Granger analyses of de-stepped (stationary) annual data for paired TWP, TEP and GMST for three climate models (1880–2100) compared to observations (1880–2018). The models are separated according to the closest date that may distinguish free from forced mode in observations.

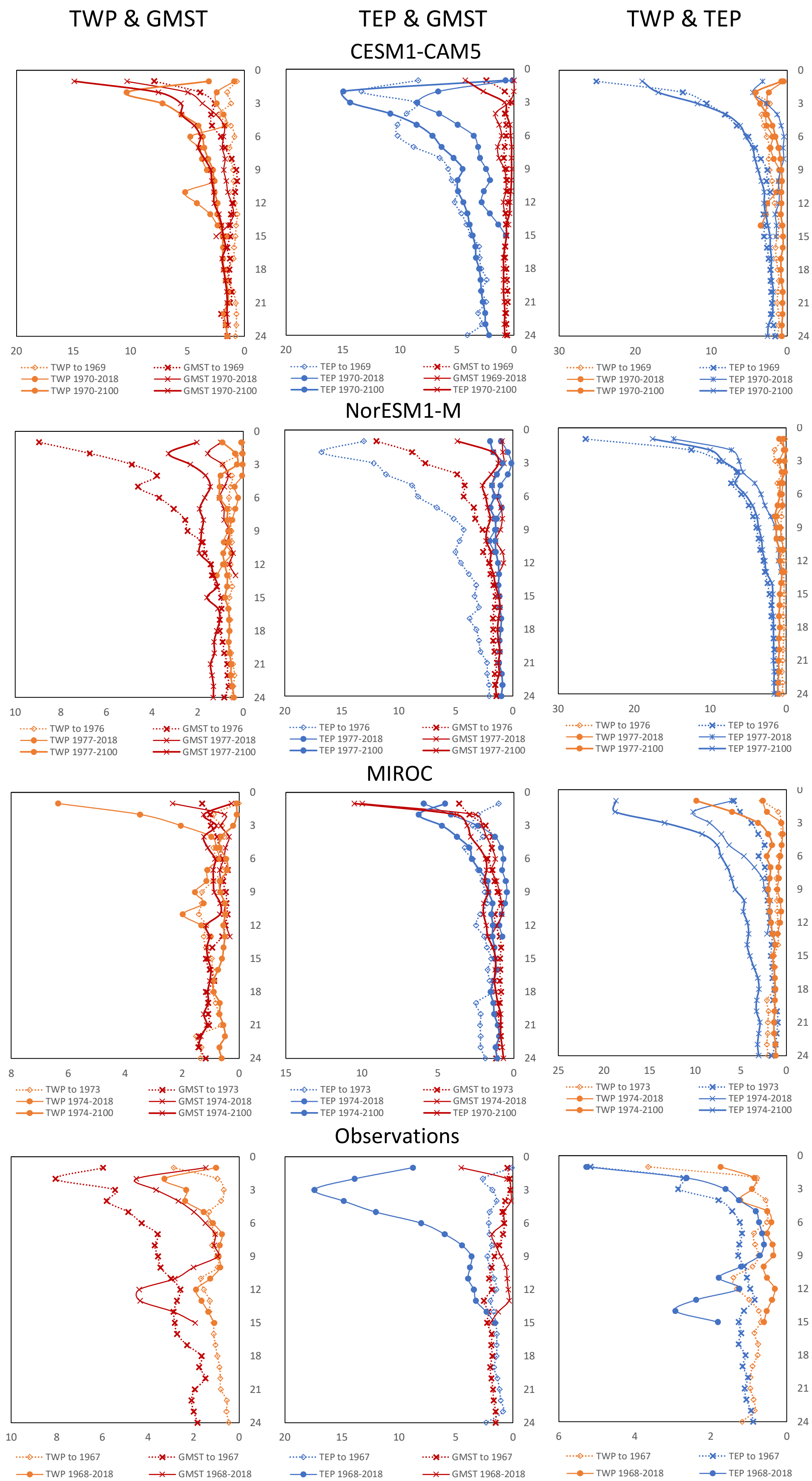

TWP & GMST
TEP & GMST
TWP & TEP
CESM1-CAM5
TWP to 1969
TWP 1970-2018
TWP 1970-2100
GMST to 1969
GMST 1970-2018
GMST 1970-2100
TEP to 1969
TEP 1970-2018
TEP 1970-2100
GMST to 1969
GMST 1969-2018
TEP 1970-2100
TWP to 1969
TWP 1970-2018
TWP 1970-2100
TEP to 1969
TEP 1970-2018
TEP 1970-2100
NorESM1-M
TWP to 1976
TWP 1977-2018
TWP 1977-2100
GMST to 1976
GMST 1977-2018
GMST 1977-2100
TEP to 1976
TEP 1977-2018
TEP 1977-2100
GMST to 1976
GMST 1977-2018
GMST 1977-2100
TWP to 1976
TWP 1977-2018
TWP 1977-2100
TEP to 1976
TEP 1977-2018
TEP 1977-2100
MIROC
TWP to 1973
TWP 1974-2018
TWP 1974-2100
GMST to 1973
GMST 1974-2018
GMST 1974-2100
TEP to 1973
TEP 1974-2018
TEP 1974-2100
GMST to 1973
GMST 1974-2018
TEP 1970-2100
TWP to 1973
TWP 1974-2018
TWP 1974-2100
TEP to 1973
TEP 1974-2018
TEP 1974-2100
Observations
TWP to 1967
TWP 1968-2018
GMST to 1967
GMST 1968-2018
TEP to 1967
TEP 1968-2018
GMST to 1967
GMST 1968-2018
TWP to 1967
TWP 1968-2018
TEP to 1967
TEP 1968-2018

S2.3. Outgoing longwave radiation

Outgoing longwave radiation analysed for shifts includes the satellite data NOAA Interpolated Outgoing Longwave Radiation (OLR, 1979–2019) and the following reanalyses: the NCAR-NCEP Reanalysis 1 (R1 1948–2019) and NOAA/CIRES/DOE 20th Century Reanalysis (V3 1836–2015). The main paper presents tropical (30 °S – 30 °N) and extratropical comparisons, noting the large difference in interannual variability between observations and reanalyses.

Comparisons between the satellite and reanalysis data are shown in in Fig. S4 and correlations are shown in Table S6. They imply meaningful statistical relationships in some instances but some are due to an overall response to forcing. The key region of the tropics shows low correlation with the reanalyses, whereas the correlations with TEP and TWP are very high. This is due to the small area and well-understood relationships between surface heat content and outward longwave radiation. If the time series are detrended, the most naïve way to produce stationarity, most correlations either decreases or stay within ±0.05 (not shown). The exception is for tropical regions in the NCAR-NCEP Reanalysis 1, partly due to their trends having opposite signs.

The global data shows an increase in 2003, which can be related to increase in specific humidity and a decrease with the change in PDO in 2015 from negative to positive (2.4 and -1.7 W m^{-2}). The is driven by a decrease in the tropics (20°S–20°N), mainly in the northern part. The only other regions where observations show notable shifts are the NH extratropics, 30–60°N in 2001 (3.1 W m^{-2}) and a minor shift in 2013 ($p<0.1$) and 60–90°N in 2002 and 2016 (4.2 and 2.2 W m^{-2}) and 90–60°S in 2003 (1.8 W m^{-2}). The tropical changes may be mostly decadal variability and the extratropical change can be related to changes in specific humidity (in main paper).

Table S6: Correlations between NOAA Interpolated Outgoing Longwave Radiation (1979–2019) and the NCAR-NCEP Reanalysis 1 and NOAA/CIRES/DOE 20th Century Reanalysis V3.

Region	Obs–R1	p value	Obs–V3	p value
Global	0.52	<0.01	0.35	<0.05
20°S–20°N	0.30		0.30	
90–60°S	0.42	<0.01	0.34	<0.05
60–30°S	0.49	<0.01	0.40	<0.05
30–0°S	0.21		0.25	
0–30°N	0.36	<0.05	0.09	
30–60°N	0.52	<0.01	0.40	<0.05
60–90°N	0.76	<0.01	0.44	<0.01
TWP	0.74	<0.01	0.72	<0.01
TEP	0.77	<0.01	0.90	<0.01
30°S–30°N	0.23		0.11	
Extratropics	0.54	<0.01	0.49	<0.01

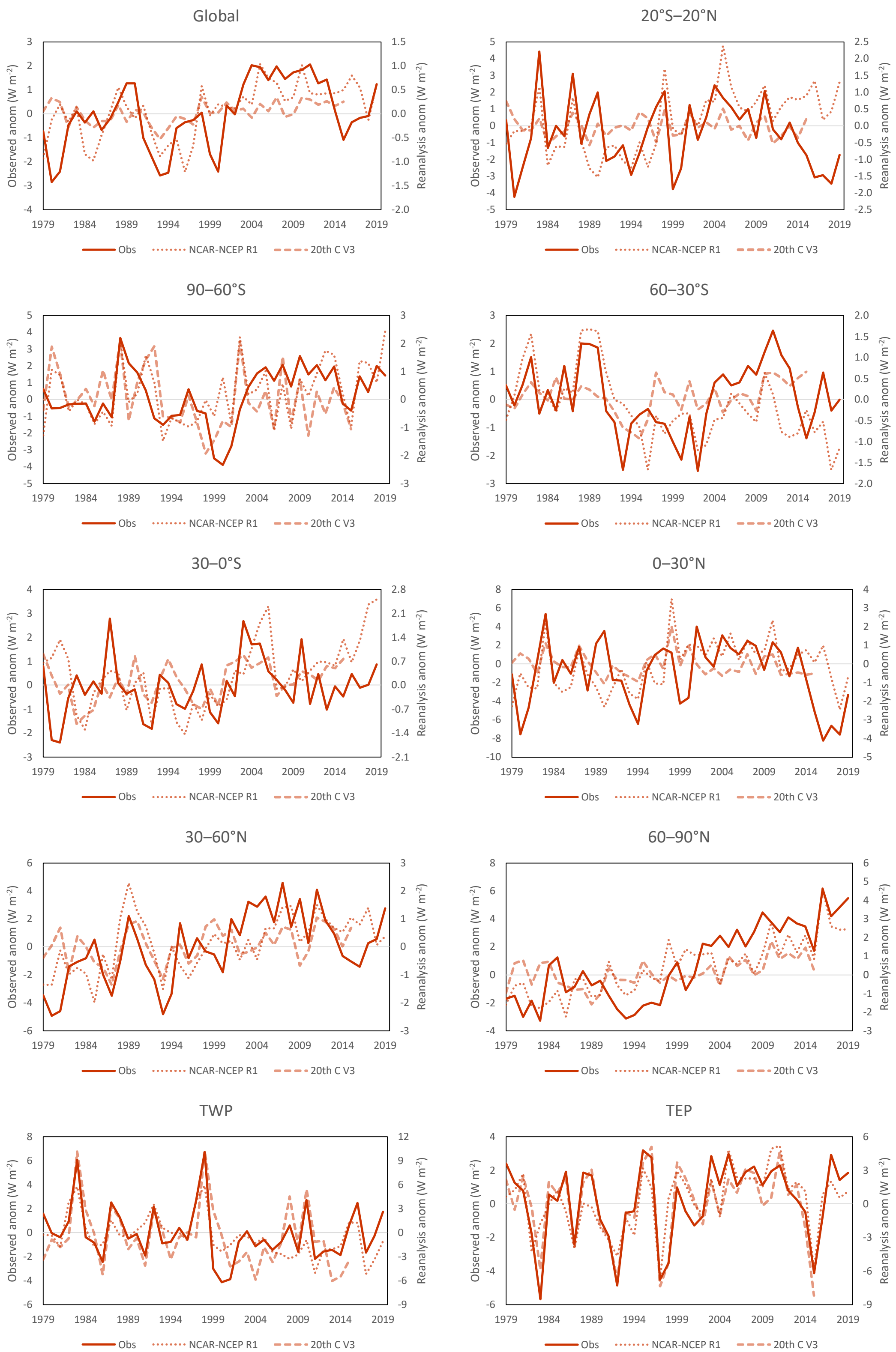

Figure S4: Comparison of observed (satellite, NOAA Interpolated Outgoing Longwave Radiation) and reanalysis (NCAR-NCEP Reanalysis 1, NOAA/CIRES/DOE 20th Century Reanalysis V3) 1979–2019 shown as a 1981–2010 anomaly for different regions.

S2.4. Specific humidity

Table S7 shows the results of step change analysis in selected values of specific humidity from the HadIDSH data in anomalies of g kg^{-1}. In general, they follow temperature by some months but broadly coincide with the observed changes shown in JR21. Fig. S5 shows a comparison of tropical and NH ocean monthly anomalies. Each peak from 1987 to 2014 has been associated with a regime change globally or within a hemisphere.

Table S7: Regime shifts in specific humidity from the HadIDSH data 1973–2010 for major land and ocean regions. Regions are 70° S – 70° N global, 20°–70° for the hemispheres and 20° S – 20° N tropics.

Region	Ti0	Year	Shift	Month	P value
Global land	9.8	1987	0.13	May-87	p<0.05
	10.0	1997	0.13	Jun-97	p<0.05
	9.4	2015	0.16	Sep-15	p<0.05
NH Land	11.0	1987	0.14	Nov-87	p<0.01
	8.8	1997	0.11	Mar-97	p<0.05
	11.7	2015	0.15	Sep-15	p<0.01
SH Land	NR				
Global ocean	22.7	1994	0.18	May-97	p<0.01
	12.2	2014	0.16	Jun-15	p<0.01
NH ocean	11.7	1988	0.14	Nov-87	p<0.01
	11.0	1994	0.09	Jul-94	p<0.01
	11.9	2014	0.11	May-14	p<0.01
SH ocean	11.8	2015	0.18	Aug-15	p<0.01
Tropical ocean	16.4	1987	0.22	Apr-87	p<0.01
	13.4	2016	0.29	Jul-15	p<0.01

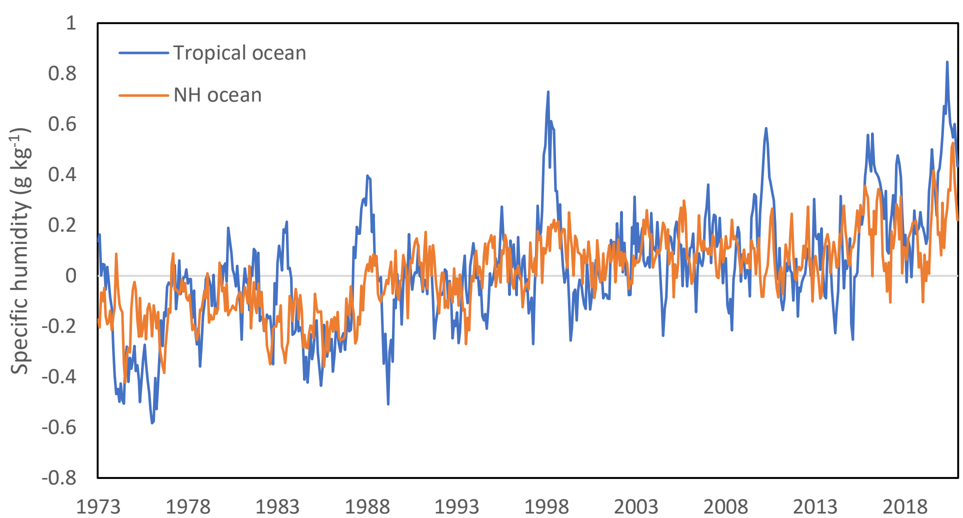

Figure S5: Comparison of specific humidity for the tropical (20° S – 20° N) and NH (20°–70°) oceans from the HadIDSH data in anomalies of g kg^{-1}.

S3. Data sources

S3.1. CMIP5 Climate model data

CMIP5 RCP4.5 model GMST records were downloaded from the KNMI data explorer web site http://climexp.knmi.nl/ 7 Jan 2015. The models used in the study are in Table S8 along with ECS estimates where available. Further details are provided in the supplementary information of Jones and Ricketts (2021). SST was extracted for TEP and TWP from 30 GCMs from the Run 1 Physics 1 simulations, the initial member of each model ensemble in February 2015.

Table S8: List of modelling groups and global climate models used for simulations of 20th and 21st century climate, available from the CMIP5 database http://cmip-pcmdi.llnl.gov/cmip5/availability.html, for RCP4.5 with run numbers 1 and physics perturbations 1 with equilibrium climate sensitivity (ECS). ECS is taken from Sherwood et al. (2014) unless otherwise noted.

Centre	Model	ECS
BoM/CSIRO, Australia	ACCESS1-0	3.79
BoM/CSIRO, Australia	ACCESS1-3	3.45
Beijing Climate Center, China	BCC-CSM1-1	2.88
Beijing Climate Center, China	BCC-CSM1-1-M	2.90
Beijing Normal University, China	BNU-ESM	4.11
Canadian Climate Centre, Canada	CanESM2	3.68
National Center for Atmospheric Research, USA	CESM1-CAM5	4.10[1]
Meteo-France, France	CNRM-CM5	3.25
CSIRO/QCCCE, Australia	CSIRO-Mk3-6-0	3.99
EC-Earth Consortium	EC-EARTH	3.4[2]
LASG/Institute of Atmospheric Physics, China	FGOALS-g2	3.45
LASG/Institute of Atmospheric Physics, China	FGOALS-s2	4.20
Geophysical Fluid Dynamics Lab, USA	GFDL-CM3	3.96
Geophysical Fluid Dynamics Lab, USA	GFDL-ESM2G	2.38
Geophysical Fluid Dynamics Lab, USA	GFDL-ESM2M	2.41
NASA/Goddard Institute for Space Studies, USA	GISS-E2-H	2.30
NASA/Goddard Institute for Space Studies, USA	GISS-E2-R	2.11
Met Office Hadley Centre, UK	HadGEM2-ES	4.55
Institut Pierre Simon Laplace, France	IPSL-CM5A-LR	4.1
Institut Pierre Simon Laplace, France	IPSL-CM5A-MR	
Institut Pierre Simon Laplace, France	IPSL-CM5B-LR	2.59
Centre for Climate Research, Japan	MIROC5	2.71
Centre for Climate Research, Japan	MIROC-ESM	4.65
Centre for Climate Research, Japan	MIROC-ESM-CHEM	
Max Planck Institute for Meteorology DKRZ, Germany	MPI-ESM-LR	3.60
Max Planck Institute for Meteorology DKRZ, Germany	MPI-ESM-MR	3.44
Meteorological Research Institute, Japan	MRI-CGCM3	2.59
Norwegian Climate Center, Norway	NorESM1-M	2.83
Norwegian Climate Center, Norway	NorESM1-ME	

1. Estimate from model developers (Meehl et al., 2013)
2. Estimate from model developers (Lacagnina et al., 2014)

Additional monthly data from the KNMI data explorer was downloaded between May-June 2020. All are from data finalised in 2011 to 2012, so the download times do not affect version control. The additional data is from models CESM1-CAM5 (Neale et al., 2013), NorESM1-M (Bentsen et al., 2013;Iversen et al., 2013) and MIROC-ESM (Watanabe et al., 2011) run1, physics 1. Regions for surface temperature downloaded include TWP, TEP, GMST, global land, global ocean, tropical ocean (20 °S–20 °N, SH 30–60 °S, NH 30–60 °N, NH land and SH land. Additionally, selected regional and global monthly means were downloaded for top of the atmosphere short- and long-wave radiation and surface latent heat and sensible heat flux for CESM1-CAM5, and top of the atmosphere short- and long-wave radiation for NorWSM1-M.

S3.2. Outgoing longwave radiation

Data sources are NOAA Interpolated Outgoing Longwave Radiation (OLR, 1979–2019)(Lee, 2014), the NCAR-NCEP Reanalysis 1 (R1 1948–2019)(Kalnay et al., 1996) and NOAA/CIRES/DOE 20th Century Reanalysis (V3 1836–2015) (Slivinski et al., 2019).

The observed data was downloaded from the NOAA Physical Sciences Laboratory (https://psl.noaa.gov/data/gridded/data.interp_OLR.html) and the NCAR-NCEP Reanalysis 1 (https://psl.noaa.gov/data/gridded/data.ncep.reanalysis.html). The 20th Century reanalysis data was downloaded from the KNMI data explorer, and spatial averages have recently also been made available from NOAA PSL (https://psl.noaa.gov/data/gridded/data.20thC_ReanV3.html). All data was downloaded in June 2020. Original data source: NOAA/OAR/ESRL PSL, Boulder, Colorado, USA.

S3.3. Specific humidity

The Hadley Centre HadISDH data set was used to investigate changes in specific humidity. The land data set is version 4.3.1.2020f (Smith et al., 2011;Willett et al., 2014) and the marine and blended data sets version 1.1.0.2020f (Willett et al., 2020). Updates to the data were downloaded in May 2021 and is the final version for the data to December 2020. (https://www.metoffice.gov.uk/hadobs/hadisdh/).

Table S9: Details of shifts produced by the multi-step bivariate test for 29 RCP4.5 GCM simulations for GMST, TEP and TWP. Matches are coloured. Probability of GMST being related to warm pool shifts calculated allowing ±1 year either side, a 7-year detection gap between shifts assuming a constant rate of shifts over time. All dates register the time period before the change. The area-weighted probability is calculated based on the area of TWP and TEP having a global influence based on being 5.7% of global surface area.

Model	Shift dates GMST	Shift dates TEP	Shift dates TWP	TEP & TWP matches	TEP & TWP shifts	GMST Shifts	Raw prob	Area-weight
ACCESS1-0	[1882,1896,1915,1986,1997,2011,2030,2048,2062,2076]	[1997,2025,2054,2074]	[1915,1996,2010,2022,2032,2042,2056,2072]	4	12	10	0.29	0.02
ACCESS1-3	[1913,1982,2000,2007,2021,2032,2045,2057,2076,2092]	[2000,2037,2050]	[1909,1995,2006,2021,2033,2045,2052,2068]	5	11	10	0.09	0.01
bcc-csm1-1	[1919,1973,1985,1995,2006,2020,2035,2053,2074]	[1919,1987,2007,2039,2078]	[1908,1925,1972,1988,2005,2025,2038,2047,2073]	5	14	9	0.26	0.01
bcc-csm1-1-m	[1906,1944,1968,1985,1997,2015,2031,2059,2076]	[1906,1995,2019]	[1907,1966,1987,2000,2016,2033,2060]	4	10	9	0.20	0.01
BNU-ESM	[1883,1913,1942,1977,1994,2005,2021,2044,2057,2077]	[1947,2005,2044]	[1912,1966,1995,2013,2024,2040,2057,2078]	6	11	10	0.03	0.002
CanESM2	[1910,1976,1995,2002,2019,2028,2035,2045,2057,2074]	[1935,2002,2020,2058]	[1911,1980,2000,2020,2035,2046,2058,2076]	8	12	10	0.01	0.0004
CCSM4	[1919,1974,1997,2013,2030,2042,2059,2080]	[1922,1997,2021,2058,2095]	[1883,1908,1931,1972,1997,2014,2027,2037,2058,2068,2095]	5	16	8	0.38	0.02
CESM1-CAM5	[1883,1914,1971,1997,2013,2028,2042,2053,2065,2080]	[1996,2029,2063]	[1916,1970,1997,2014,2030,2037,2051,2067,2080]	6	12	10	0.12	0.01
CNRM-CM5	[1892,1902,1935,1985,2001,2024,2037,2050,2059,2070,2082]	[1989,2013,2050]	[1920,1986,2000,2024,2039,2051,2070]	6	10	11	0.06	0.003
CSIRO-Mk3-6-0	[1914,1940,1960,1996,2015,2034,2050,2065,2077]	[1911,2010,2034,2048,2066]	[1911,1997,2016,2035,2050,2071]	6	11	9	0.04	0.002
EC-EARTH	[1907,1919,1975,1986,1997,2014,2026,2037,2052,2063,2083]	[1919,1975,1997,2017,2039,2054]	[1883,1908,1928,1976,1995,2005,2021,2040,2062,2088]	6	16	11	0.31	0.02
FGOALS-g2	[1927,1964,1977,1995,2012,2024,2035,2051,2065]	[1968,2000,2024]	[1912,1969,1988,2000,2014,2025,2036,2054]	3	11	9	0.43	0.02
GFDL-CM3	[1867,1883,1919,1933,1962,1977,1996,2008,2021,2036,2050,2066,2082]	[1996,2021,2048]	[1883,1921,1941,1963,1977,2000,2017,2038,2049,2058,2081]	7	14	13	0.16	0.01
GFDL-ESM2G	[1914,1930,1984,1996,2022,2045]	[1901,1994,2045]	[1908,1973,1996,2016,2038,2050]	2	9	6	0.21	0.01
GFDL-ESM2M	[1883,1893,1976,1995,2010,2027,2040,2059]	[1909,1999,2044]	[1883,1908,1976,1999,2011,2027,2050,2058]	5	11	8	0.03	0.002
GISS-E2-H	[1905,1917,1932,1972,1994,2001,2014,2022,2034,2046,2056,2063,2080]	[1928,1973,2000,2012,2034,2050]	[1905,1931,1994,2014,2031,2048,2063]	8	13	13	0.05	0.003
GISS-E2-R	[1924,1972,1997,2009,2023,2033,2045,2060,2094]	[1909,1973,1998,2016,2035,2063]	[1911,1962,1971,1999,2013,2022,2036,2062]	4	14	9	0.42	0.02
HadGEM2-ES	[1915,1936,1953,1984,1997,2006,2015,2029,2041,2055,2070]	[1913,2006,2041,2068]	[1904,1997,2006,2017,2031,2042,2056,2069]	7	12	11	0.09	0.01
IPSL-CM5A-LR	[1921,1972,1986,1996,2009,2017,2030,2046,2061,2090]	[1921,1997,2028,2046,2061]	[1922,1987,1997,2013,2029,2044,2061,2090]	10	13	10	0.001	0.00003
IPSL-CM5A-MR	[1905,1926,1976,1995,2008,2022,2042,2056,2067,2075]	[1934,1979,2008,2022,2057,2075]	[1914,1934,1979,1995,2008,2022,2029,2049,2057,2070]	7	16	10	0.16	0.01
IPSL-CM5B-LR	[1883,1904,1936,1961,1970,1996,2011,2026,2035,2055,2075]	[1904,1986,2022,2055]	[1905,1922,1971,1997,2017,2035,2060]	6	11	11	0.09	0.01
MIROC5	[1920,1996,2019,2036,2064]	[2002,2041]	[1906,1998,2024,2036,2068]	1	7	5	0.36	0.02
MIROC-ESM	[1921,1942,1963,1975,1995,2009,2020,2033,2045,2057,2070]	[1919,1942,1995,2020,2031,2057,2071]	[1922,1974,1995,2010,2021,2031,2057]	11	14	11	0.004	0.0002
MIROC-ESM-CHEM	[1917,1975,1995,2007,2023,2040,2048,2055,2071,2081]	[1910,1974,2004,2024,2049,2071]	[1916,1977,2006,2023,2048,2055,2072]	10	13	10	0.02	0.001
MPI-ESM-LR	[1908,1970,1997,2010,2027,2036,2061]	[1971,2010,2049]	[1881,1908,1971,1998,2010,2031,2049,2073]	6	11	7	0.03	0.002
MPI-ESM-MR	[1883,1891,1919,1970,1988,1996,2006,2021,2039,2048,2073]	[1944,1996,2015,2040]	[1919,1970,1996,2007,2024,2040,2059]	6	11	11	0.09	0.01
MRI-CGCM3	[1882,1907,1933,1975,2001,2020,2037,2046,2068,2080]	[1987,2019,2043,2063]	[1883,1907,1995,2008,2025,2040,2048,2060,2068]	4	13	10	0.28	0.02
NorESM1-M	[1909,1976,1998,2011,2022,2037,2056,2070,2088]	[1933,2002,2035,2059]	[1883,1910,1934,1984,1997,2018,2037,2057,2089]	5	13	9	0.10	0.01
NorESM1-ME	[1923,1977,1999,2012,2026,2039,2049,2067,2083]	[2001,2045]	[1908,1972,1998,2013,2023,2040,2050,2062,2088]	4	11	9	0.14	0.01

Table S10: Correlations between CMIP5 model skill scores (Fasullo, 2020;Fasullo et al., 2020) and heat engine metrics divided into models with ECS <3.5 °C (n=11) and those with ECS >3.5 °C (n=10). Correlations p<0.05 are shown in bold.

	ECS	Overall	Energy	Water	Dynamics	Annual	Seasonal	ENSO	PRW	SLP	LWNet toa	Z500	RH500	SWNet toa	LH	Usfc	LWcf	Rt-Fs	P	E-P	SWcf	Fs	RHsfc	W500
ECS (°C)	<3.5 °C	0.55	0.41	0.59	0.58	0.49	0.42	0.40	0.42	0.53	0.48	**0.61**	0.38	0.31	**0.71**	0.55	0.44	0.32	**0.60**	0.54	0.36	0.22	0.02	0.47
	>3.5 °C	0.27	0.32	0.42	0.14	0.15	0.06	0.41	0.58	-0.09	0.61	-0.12	0.19	0.33	0.17	0.07	0.52	0.09	0.43	0.47	0.19	-0.02	-0.28	0.27
TEP av (°C)	<3.5 °C	0.56	0.45	0.48	**0.61**	0.58	0.54	0.37	0.50	0.31	0.48	0.56	0.53	0.25	0.46	0.40	0.57	0.48	0.39	0.35	0.43	0.34	0.17	**0.60**
	>3.5 °C	0.40	0.48	0.34	0.32	0.21	0.42	0.37	0.52	-0.10	0.49	-0.15	0.48	0.49	0.15	-0.01	0.43	0.54	0.32	0.23	0.42	0.26	0.05	0.45
TWP av (°C)	<3.5 °C	-0.26	-0.34	-0.43	-0.01	0.23	0.31	-0.46	-0.43	-0.21	-0.18	-0.04	0.02	-0.45	-0.45	-0.07	-0.21	-0.13	-0.30	-0.47	-0.34	-0.41	-0.12	0.08
	>3.5 °C	**-0.89**	**-0.80**	**-0.86**	**-0.90**	**-0.75**	**-0.82**	**-0.79**	-0.53	-0.47	-0.43	**-0.68**	**-0.84**	**-0.85**	**-0.86**	-0.56	-0.43	-0.59	**-0.84**	**-0.85**	**-0.88**	-0.65	0.17	**-0.87**
TWP-TEP	<3.5 °C	-0.48	-0.42	-0.28	-0.55	-0.46	**-0.65**	-0.27	-0.35	-0.30	-0.41	-0.49	**-0.61**	-0.30	-0.26	-0.29	-0.04	**-0.71**	-0.14	-0.11	-0.36	-0.42	-0.49	-0.50
	>3.5 °C	**0.89**	**0.84**	**0.87**	**0.86**	**0.81**	0.65	**0.85**	0.66	0.64	0.53	**0.80**	0.66	**0.81**	**0.92**	0.43	0.58	0.48	**0.85**	**0.86**	**0.84**	**0.78**	-0.40	**0.82**
TEP shifts (n)	<3.5 °C	**-0.76**	**-0.73**	**-0.72**	**-0.70**	-0.53	-0.55	**-0.64**	**-0.74**	-0.44	**-0.62**	**-0.65**	**-0.63**	-0.57	**-0.66**	-0.51	-0.58	**-0.72**	-0.55	-0.54	**-0.72**	**-0.67**	-0.41	**-0.62**
	>3.5 °C	-0.71	-0.77	-0.67	-0.63	-0.56	-0.57	-0.71	-0.76	-0.25	-0.75	-0.23	-0.63	**-0.72**	-0.52	-0.04	**-0.76**	-0.58	-0.66	-0.57	-0.64	-0.63	0.20	**-0.73**
TWP shifts (n)	<3.5 °C	0.34	0.27	0.41	0.31	0.20	-0.10	0.34	0.26	0.31	0.36	0.34	0.30	0.26	0.31	-0.07	0.44	-0.06	0.39	0.47	0.25	0.06	0.20	0.32
	>3.5 °C	0.21	0.09	0.06	0.34	0.17	0.52	-0.02	-0.27	0.08	-0.41	0.29	0.44	0.21	0.30	0.57	-0.42	0.23	0.03	0.04	0.35	0.11	0.16	0.23
TEP hits (n)	<3.5 °C	**-0.65**	**-0.62**	-0.49	**-0.71**	-0.55	-0.42	-0.52	-0.51	**-0.70**	**-0.60**	**-0.79**	**-0.61**	-0.55	-0.56	-0.44	-0.40	-0.45	-0.35	-0.39	-0.58	**-0.61**	-0.32	-0.52
	>3.5 °C	-0.34	-0.44	-0.42	-0.22	-0.38	0.05	-0.50	-0.63	-0.37	-0.66	-0.28	0.00	-0.29	-0.36	0.18	**-0.72**	0.00	-0.43	-0.42	-0.20	-0.44	0.52	-0.28
TWP hits (N)	<3.5 °C	-0.16	-0.25	-0.16	-0.13	-0.14	-0.16	-0.16	-0.22	-0.12	-0.03	-0.08	-0.09	-0.17	-0.09	-0.05	-0.16	-0.19	0.02	0.02	-0.30	-0.44	-0.39	-0.10
	>3.5 °C	-0.65	**-0.75**	-0.65	-0.54	-0.53	-0.38	**-0.72**	**-0.77**	-0.33	**-0.75**	-0.32	-0.44	-0.66	-0.55	0.18	**-0.80**	-0.42	-0.66	-0.59	-0.58	**-0.68**	0.45	-0.64
TEP SWR	<3.5 °C	-0.56	**-0.64**	-0.60	-0.29	0.08	0.18	**-0.74**	**-0.77**	-0.23	-0.53	-0.33	-0.31	**-0.71**	-0.59	-0.28	-0.52	-0.48	-0.39	**-0.65**	**-0.64**	**-0.70**	-0.03	-0.20
	>3.5 °C	-0.62	-0.65	-0.52	-0.59	-0.29	**-0.76**	-0.52	-0.41	0.10	-0.33	-0.07	**-0.82**	**-0.76**	-0.46	-0.05	-0.28	**-0.70**	-0.54	-0.46	**-0.74**	-0.42	0.07	**-0.70**
TWP SWR	<3.5 °C	-0.14	-0.35	-0.08	0.09	0.40	0.52	-0.44	-0.40	-0.14	-0.22	-0.10	0.11	-0.54	-0.24	-0.23	-0.19	-0.08	0.01	-0.24	-0.38	-0.59	0.49	0.28
	>3.5 °C	-0.13	-0.08	-0.12	-0.19	-0.13	-0.23	-0.07	-0.11	-0.06	0.04	-0.16	-0.21	-0.11	-0.24	0.07	-0.02	0.43	-0.18	-0.23	-0.18	0.00	**0.87**	-0.20
GMST hits %	<3.5 °C	-0.33	-0.34	-0.32	-0.33	-0.35	-0.46	-0.21	-0.26	-0.09	-0.21	-0.22	-0.30	-0.17	-0.18	-0.09	-0.18	-0.45	-0.22	-0.11	-0.36	-0.30	-0.46	-0.38
	>3.5 °C	-0.49	-0.56	-0.47	-0.42	-0.54	-0.22	-0.54	-0.66	-0.46	-0.63	-0.38	-0.22	-0.41	-0.48	0.10	**-0.73**	-0.06	-0.47	-0.42	-0.37	-0.60	0.63	-0.46
TEP&TWP hits (%)	<3.5 °C	-0.43	-0.49	-0.37	-0.41	-0.33	-0.35	-0.38	-0.44	-0.34	-0.29	-0.39	-0.33	-0.39	-0.36	-0.31	-0.28	-0.46	-0.15	-0.17	-0.52	**-0.66**	-0.43	-0.31
	>3.5 °C	-0.56	**-0.67**	-0.58	-0.42	-0.55	-0.15	**-0.68**	**-0.77**	-0.46	**-0.82**	-0.37	-0.20	-0.51	-0.52	0.09	**-0.88**	-0.30	-0.57	-0.52	-0.41	**-0.69**	0.37	-0.49
Total hits (%)	<3.5 °C	**-0.83**	**-0.78**	**-0.81**	**-0.76**	-0.56	-0.48	**-0.72**	**-0.77**	-0.52	**-0.71**	**-0.73**	**-0.69**	-0.63	**-0.72**	-0.45	**-0.68**	-0.66	-0.65	-0.67	**-0.76**	-0.64	-0.45	**-0.68**
	>3.5 °C	**-0.78**	**-0.77**	**-0.67**	**-0.78**	-0.58	**-0.87**	-0.65	-0.57	-0.20	-0.46	-0.32	**-0.89**	**-0.82**	-0.62	-0.27	-0.45	-0.65	-0.66	-0.59	**-0.83**	-0.59	0.19	**-0.84**
P values	<3.5 °C	**-0.74**	**-0.67**	**-0.77**	-0.65	-0.47	-0.43	-0.65	**-0.73**	-0.38	-0.60	-0.59	-0.56	-0.53	**-0.71**	-0.45	-0.63	-0.63	-0.59	-0.63	-0.66	-0.59	-0.37	-0.61
	>3.5 °C	**-0.90**	**-0.85**	**-0.83**	**-0.89**	**-0.69**	**-0.89**	**-0.79**	**-0.66**	-0.32	-0.53	-0.47	**-0.93**	**-0.90**	**-0.75**	-0.42	-0.51	**-0.70**	**-0.82**	**-0.78**	**-0.91**	-0.63	0.18	**-0.93**

PRW precipitable water, SLP sea level pressure, LWNet toa, top-of-atmosphere net longwave radiation, Z500 500 hPa geopotential height, 500 hPa relative humidity, LWNet toa, top-of-atmosphere net shortwave radiation, LH latent heat, Usfc surface-adjusted windspeed, LWcf cloud-forced longwave radiation, Rt-Fs total energy input toa downward minus surface upward, P precipitation, E-P evaporation-precipitation deficit, SWcf shortwave cloud forcing, Fs surface energy flux, RHsfc surface relative humidity, W500 vertical velocity at 500 hPa. SWR shift warming ratio.

Plates 1-3: Tracking model results for CESM1-CAM5 (1), NorESM1-M (2) and MIROC-ESM (3). Top: destepped TWP monthly data showing exceedances of 0.3, 0.2 and 0.3 °C respectively with TWP and TEP shifts; second: TWP (orange) and TEP (blue) monthly data with running means showing provisional (dotted) and confirmed (solid) shifts; Third: as for above with GMST (red), land (green) and ocean (blue); Bottom: patterns of shift dates for the ten regions analysed. All measurements, anomalies in °C.

Plate 1 CESM-CAM5

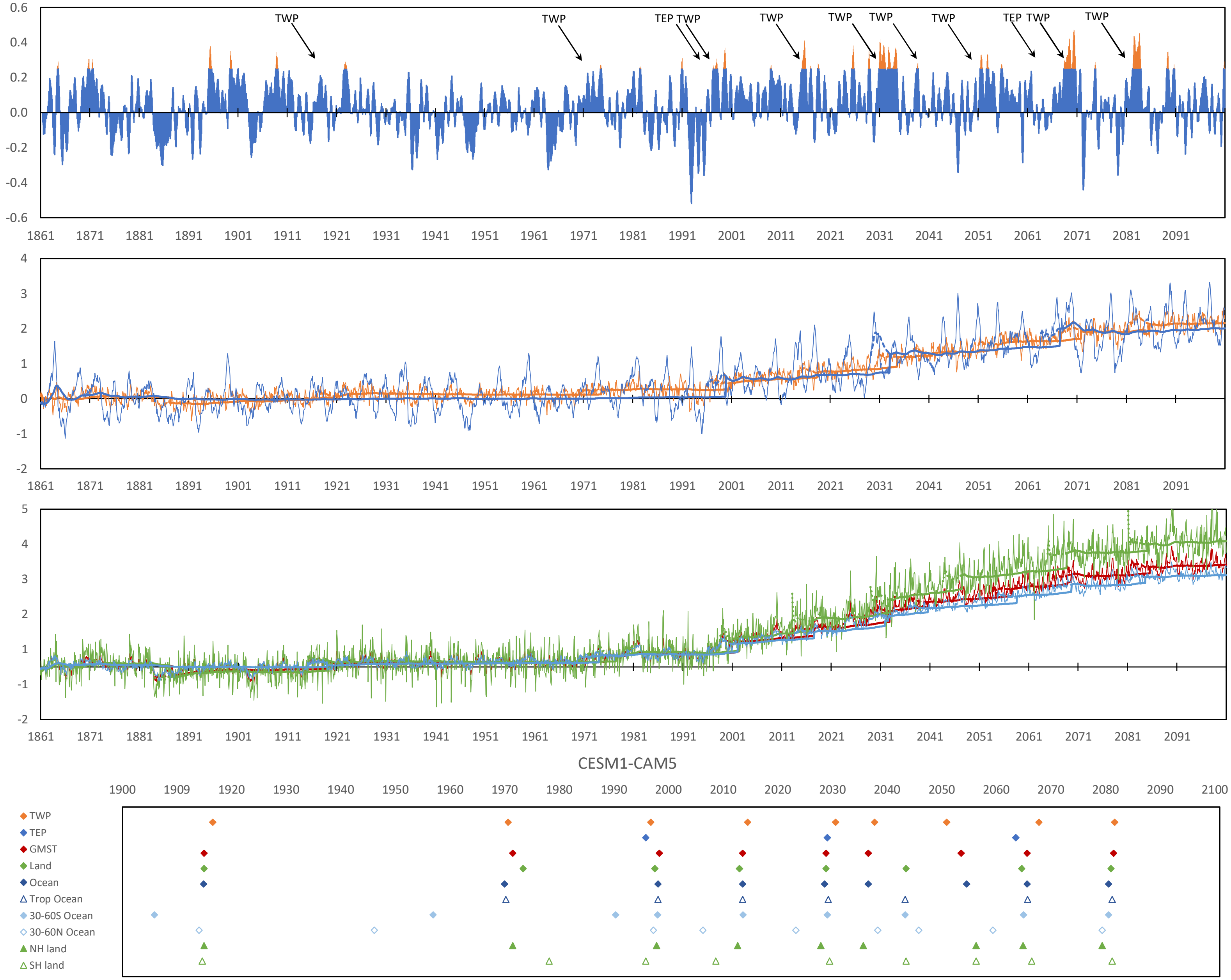

Plate 2 Nor-ESM

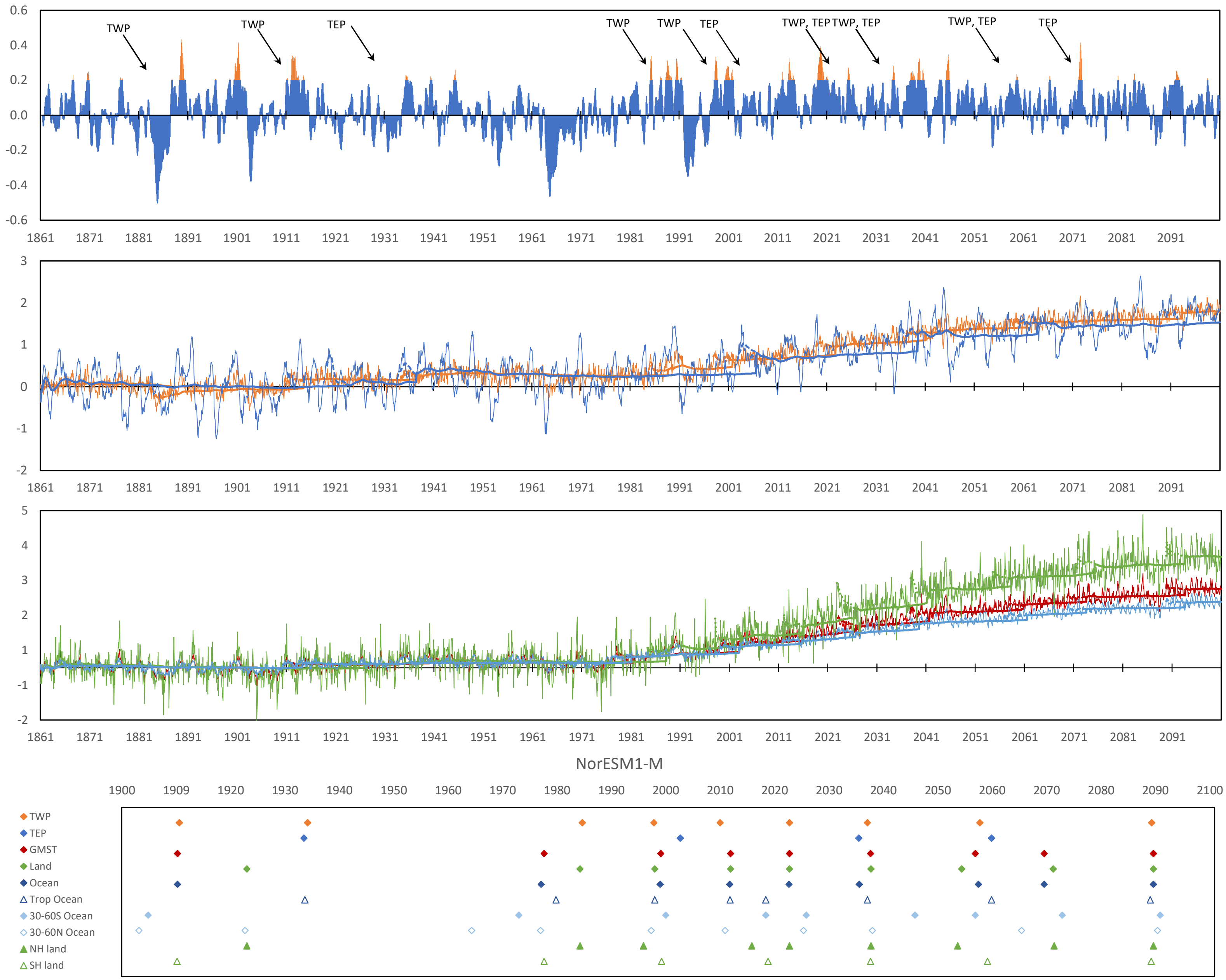

Plate 3 MIROC-ESM

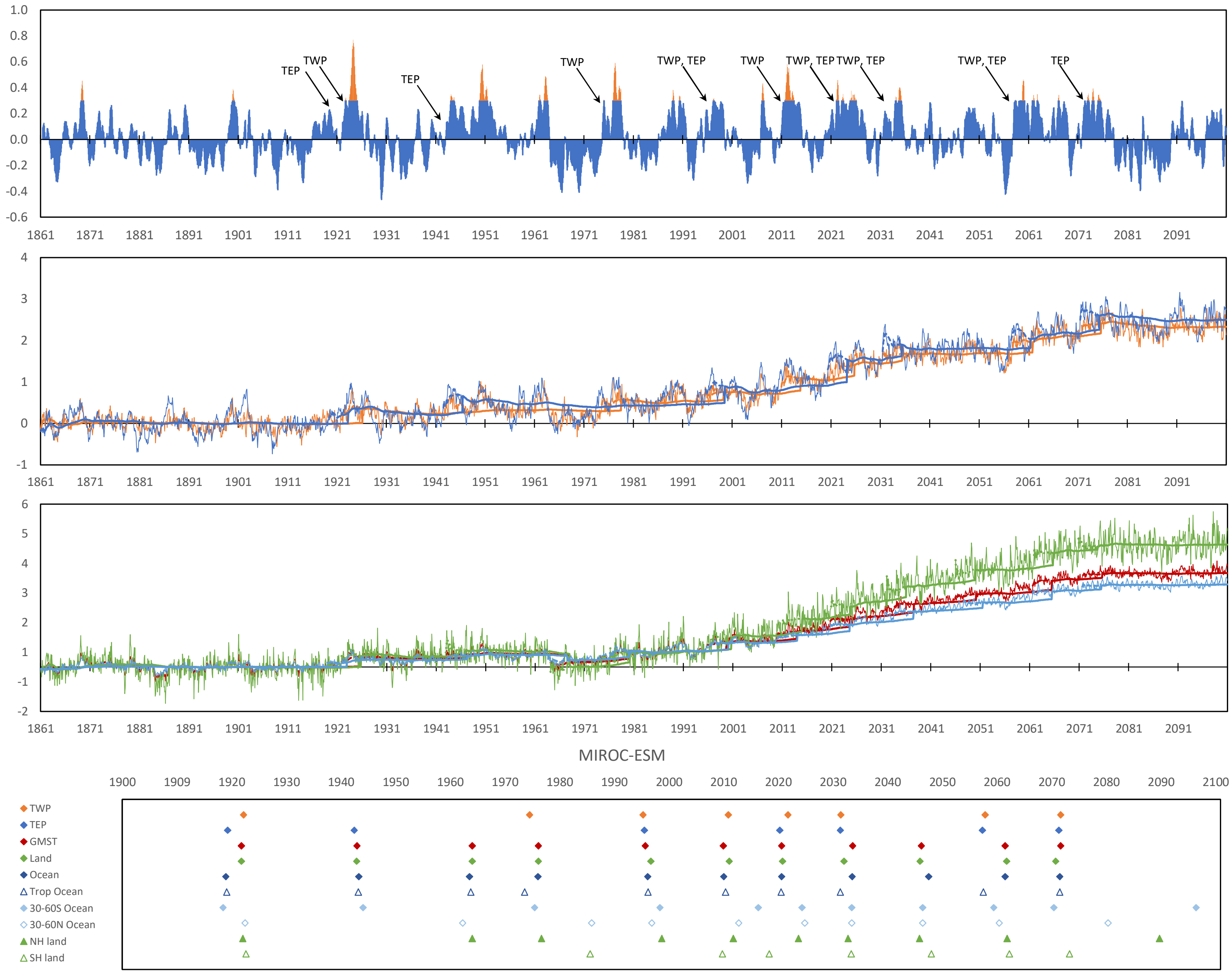

References

Bentsen, M., Bethke, I., Debernard, J. B., Iversen, T., Kirkevåg, A., Seland, Ø., Drange, H., Roelandt, C., Seierstad, I. A., and Hoose, C.: The Norwegian Earth System Model, NorESM1-M–Part 1: description and basic evaluation of the physical climate, Geosci Model Dev, 6, 687-720, 2013.
Fasullo, J. T.: Evaluating Simulated Climate Patterns from theCMIP Archives Using Satellite and Reanalysis Datasets, Geosci Model Dev Discuss, 2020, 1-26, 10.5194/gmd-2020-1, 2020.
Fasullo, J. T., Phillips, A. S., and Deser, C.: Evaluation of Leading Modes of Climate Variability in the CMIP Archives, J Clim, 33, 5527-5545, 10.1175/jcli-d-19-1024.1, 2020.
Iversen, T., Bentsen, M., Bethke, I., Debernard, J., Kirkevåg, A., Seland, Ø., Drange, H., Kristjansson, J., Medhaug, I., and Sand, M.: The Norwegian earth system model, NorESM1-M–Part 2: climate response and scenario projections, Geosci Model Dev, 6, 389-415, 2013.
Jones, R. N., and Ricketts, J. H.: Reconciling the signal and noise of atmospheric warming on decadal timescales, Earth Syst Dyn, 8, 177-210, 10.5194/esd-8-177-2017, 2017.
Jones, R. N., and Ricketts, J. H.: The Pacific Ocean heat engine, Earth Syst Dyn, submitted, 2021.
Kalnay, E., Kanamitsu, M., Kistler, R., Collins, W., Deaven, D., Gandin, L., Iredell, M., Saha, S., White, G., and Woollen, J.: The NCEP/NCAR 40-year reanalysis project, Bull Am Meteorol Soc, 77, 437-472, 1996.
Lacagnina, C., Selten, F., and Siebesma, A. P.: Impact of changes in the formulation of cloud-related processes on model biases and climate feedbacks, J Adv Model Earth Syst, 6, 1224-1243, https://doi.org/10.1002/2014MS000341, 2014.
Lee, H.: Climate algorithm theoretical basis document (C-ATBD): Outgoing longwave radiation (OLR)—Daily. NOAA's Climate Data Record (CDR) Program, 46, 2014.
Meehl, G. A., Washington, W. M., Arblaster, J. M., Hu, A., Teng, H., Kay, J. E., Gettelman, A., Lawrence, D. M., Sanderson, B. M., and Strand, W. G.: Climate Change Projections in CESM1(CAM5) Compared to CCSM4, J Clim, 26, 6287-6308, https://doi.org/10.1175/JCLI-D-12-00572.1, 2013.
Neale, R. B., Richter, J., Park, S., Lauritzen, P. H., Vavrus, S. J., Rasch, P. J., and Zhang, M.: The mean climate of the Community Atmosphere Model (CAM4) in forced SST and fully coupled experiments, J Clim, 26, 5150-5168, 2013.
Ricketts, J., and Jones, R.: Characterizing change-points in climate series with a severe approach, MODSIM2017, 22nd International Congress on Modelling and Simulation, Hobart, Tasmania, 2018.
Ricketts, J. H.: A probabilistic approach to climate regime shift detection based on Maronna's bivariate test, The 21st International Congress on Modelling and Simulation (MODSIM2015), Gold Coast, Queensland, Australia, 2015.
Ricketts, J. H.: Understanding the Nature of Abrupt Decadal Shifts in a Changing Climate, Ph D (accepted under revision), Institute of Sustainable Industry and Liveable Cities, Victoria University, Melbourne, 2019.
Slivinski, L. C., Compo, G. P., Whitaker, J. S., Sardeshmukh, P. D., Giese, B. S., McColl, C., Allan, R., Yin, X., Vose, R., Titchner, H., Kennedy, J., Spencer, L. J., Ashcroft, L., Brönnimann, S., Brunet, M., Camuffo, D., Cornes, R., Cram, T. A., Crouthamel, R., Domínguez-Castro, F., Freeman, J. E., Gergis, J., Hawkins, E., Jones, P. D., Jourdain, S., Kaplan, A., Kubota, H., Blancq, F. L., Lee, T.-C., Lorrey, A., Luterbacher, J., Maugeri, M., Mock, C. J., Moore, G. W. K., Przybylak, R., Pudmenzky, C., Reason, C., Slonosky, V. C., Smith, C. A., Tinz, B., Trewin, B., Valente, M. A., Wang, X. L., Wilkinson, C., Wood, K., and Wyszyński, P.: Towards a more reliable historical reanalysis: Improvements for version 3 of the Twentieth Century Reanalysis system, Q J R Meteorolog Soc, 145, 2876-2908, https://doi.org/10.1002/qj.3598, 2019.
Smith, A., Lott, N., and Vose, R.: The integrated surface database: Recent developments and partnerships, Bull Am Meteorol Soc, 92, 704-708, 2011.
Watanabe, S., Hajima, T., Sudo, K., Nagashima, T., Takemura, T., Okajima, H., Nozawa, T., Kawase, H., Abe, M., and Yokohata, T.: MIROC-ESM 2010: Model description and basic results of CMIP5-20c3m experiments, Geosci Model Dev, 4, 845-872, 2011.

Willett, K., Dunn, R., Thorne, P., Bell, S., De Podesta, M., Parker, D., Jones, P., and Williams Jr, C.: HadISDH land surface multi-variable humidity and temperature record for climate monitoring, Clim Past, 10, 2014.
Willett, K. M., Dunn, R. J., Kennedy, J. J., and Berry, D. I.: Development of the HadISDH. marine humidity climate monitoring dataset, Earth Syst Sci Data, 12, 2853-2880, 2020.